www.sciencemag.org/cgi/content/full/315/5818/1565/DC1

Supporting Online Material for

A Cytochrome c Oxidase Model Catalyzes Oxygen to Water Reduction Under Rate-Limiting Electron Flux

James P. Collman,* Neal K. Devaraj, Richard A. Decreau, Ying Yang, Yi-Long Yan, Wataru Ebina, Todd A. Eberspacher, Christopher E. D. Chidsey*

*To whom correspondence should be addressed. E-mail: jpc@stanford.edu (J.P.C.); chidsey@stanford.edu (C.E.D.C.)

Published 16 March 2007, *Science* **315**, 1565 (2007)
DOI: 10.1126/science.1135844

This PDF file includes:

A Cytochrome *c* Oxidase Model Catalyzes the Four Electron Reduction of Oxygen Under Rate-Limiting Electron Flux

James P. Collman*, Neal K. Devaraj, Richard A. Decreau, Ying Yang, Yi-Long Yan, Wataru Ebina, Todd A. Eberspacher, Christopher E. D. Chidsey*

Department of Chemistry, Stanford University, Stanford, California, 94305-5080.

Supporting Information

Materials and Methods

Reagents

Ethanol, decanethiol, hexadecanethiol, dimethylsulfoxide (DMSO), sodium perchlorate (anhydrous), tween-20, and copper(II) sulfate pentahydrate were purchased from commercial sources and used as received.

The synthesis of 1-azido-hexadecan-16-thiol, azidophenyleneethynylenebenzyl thiol (N_3(PEB)SH)), and ethynylferrocene have been reported elsewhere (*S1*).

Tris-(benzyltriazolylmethyl)amine (TBTA) was received as a gift from Timothy Chan (Sharpless group, Scripps Research Insitute). The copper(II) complex was prepared by adding copper(II) sulfate pentahydrate to a DMSO solution of the *tris*-(benzyltriazolylmethyl)amine (TBTA).

The syntheses of the free-base precursors of models **1a** and **2a** follow a general synthetic route used for previous models. The alkyne-containing imidazole synthon was prepared by Sonogashira coupling with an iodo-containing imidazole and trimethylsilylacetylene. The synthesis methodology, the purification, metallation, and characterization techniques used for the models were as previously described (*S2*-*S5*). The characterization data for models **1a** and **2a** are reported below.

Model 1a

^{1}H NMR ($CDCl_3$:CD_3CN:THF-d_8/1 atm CO) δ 9.07 (d, 1H, J = 8.0 Hz), 8.69-8.78 (m, 6H), 8.63-8.61 (m, 2H), 8.53 (d, 1H, J = 8.5 Hz), 8.50 (d, 1H, J = 8.5 Hz), 8.46 (d, 1H, J = 8.5 Hz), 8.23-8.29 (m, 3H), 8.18 (d, 1H, J = 7.5 Hz), 7.66-7.82 (m, 7H), 7.42-7.55 (m, 5H), 7.38 (s, 1H), 7.11 (m, 3H), 7.00 (m, 2H), 7.01 (m, 2H), 6.96 (s, 1H), 6.66 (t, 1H, J = 7.5 Hz), 6.56-6.61 (m, 2H), 5.90 (d, 2H, J = 8.5 Hz), 5.57 (s, 1H), 5.32 (s, 1H), 5.10 (s, 1H), 4.10 (s, 1H), 3.98 (s, 2H), 3.52 (s, 3H), 3.37 (s, 3H), 2.25 (s, 1H), 2.19 (s, 1H), 1.30 (s, 1H). HR-MS (ESI^+): *m/z* = 1477.3351 $[M\text{-}PF_6]^+$ (Calcd for $C_{83}H_{58}CuFeN_{16}O_5 - PF_6$: 1477.3521).

Model 2a

^{1}H NMR (THF-d_8/MeCN-d_3/$CDCl_3$ (9:1:3 vol.)/1 atm CO): δ 9.05 (d, 1H, J = 8.4 Hz), 8.78 (d, 1H, 4.0 Hz), 8.72 (t, 2H, J = 5.0 Hz), 8.69-8.67 (m, 3H), 8.58 (m, 2H), 8.47 (d, 1H, J = 8.5 Hz), 8.38 (t, 2H, J = 8.5 Hz), 8.23 (d, 1H, J = 7.0 Hz), 8.14 (d, 1H, J = 7.5 Hz), 8.05 (s, 1H), 8.03 (d, 1H, J = 7.5 Hz), 7.83-7.66 (m, 8H), 7.55 (t, 1H, J = 7.5 Hz), 7.49-7.45 (m, 3H), 7.27 (t, 1H, J = 8.0 Hz), 7.06 (s, 1H), 7.01 (t, 1H, J = 7.5 Hz), 6.98-6.87 (m, 6H), 6.80 (t, 1H, J = 7.5 Hz), 6.57 (d, 1H, J = 7.5 Hz), 5.86 (d, 2H, J = 8.0 Hz), 5.54 (s, 1H), 5.30 (s, 1H), 5.19 (s, 1H), 4.05 (s, 1H), 3.95 (s, 2H), 3.57 (s, 3H), 3.42 (s, 3H), 3.39 (s, 3H), 2.20 (s, 1H), 2.15 (s, 1H), 1.41 (s, 1H). HR-MS (ESI^+): *m/z* = 1491.3596 $[M\text{-}PF_6]^+$ (Calcd for $C_{84}H_{60}CuFeN_{16}O_5 - PF_6$: 1491.3678).

ESR Experiments

The microwave power was 10.08 mW; microwave frequency: 9.3075 GHz, modulation frequency: 100.0 kHz; modulation amplitude: 20.0 G, Receiver gain: $5.02x10^3$; Resolution in X: 1024; T = 77K. The sample was prepared at -80°C/-40°C in DMF and the EPR spectrum was recorded at 77K ($l N_2$).

Substrates

Planar gold substrates were prepared by electron-beam evaporation of a titanium adhesion layer (99.99% purity) followed by gold (99.99% purity) onto 4-inch silicon wafers. Silicon was pre-cleaned for 10 minutes in hot piranha (1 vol 30% by mass aqueous H_2O_2 : 3 vol H_2SO_4), and rinsed in deionized water (**Warning**: Piranha solution reacts violently, even explosively, with organic materials. It should not be stored or combined with significant quantities of organic material).

The deposition was carried out in a cryogenically pumped deposition chamber. Titanium thicknesses (monitored with a quartz oscillator) were on the order of 5-10 nm and gold thicknesses were on the order of 50-100nm. After deposition, the chamber was backfilled with argon.

Gold disk electrodes used in the rotating-ring-disk experiments were made from titanium disks (4mm height, 5mm diameter). Although a variety of polishing procedures produced satisfactory results, the best results were obtained when the surfaces of these disks were mechanically polished using the following procedure (Ryan MacDonald and Tim Brand, Ginzton Crystal Shop, Stanford University)

1. Mount titanium disks onto flat glass tool/chuck (approx. 3" diameter x 2 cm thick) using appropriate blocking wax. Space the individual disks evenly over the surface of the tool.
2. Rough grind the block on a cast iron plate using various sizes of alumina polishing compound (30μm to 9μm) until all samples are cleared coplanar.
3. Fine grind the block on a glass plate using various sizes of alumina polishing compound (9μM to 5μM).

4. Clean disks thoroughly to remove all alumina
5. Polish using colloidal silica slurry (Eminess 500S) against a urethane polishing pad (Rodel Suba 500) for as long as necessary to remove all surface defects.
6. Rinse block with deionized water, heat to demount titanium samples and clean in a warm bath of isopropanol.

This procedure produced a surface with a mirror finish. Polished electrodes were washed with ethanol and water, dried, and mounted in an electron beam evaporator. Titanium and gold evaporation were then carried out in a manner identical to that described above for planar gold substrates on silicon wafers. In order to reuse the disk electrodes, a used gold electrode was treated with dilute aqua regia solution (3:1:6 $HCl:HNO_3:H_2O$) until all evaporated gold was stripped off. The electrodes were then cleaned with ethanol and water, dried, and the evaporation procedure was repeated.

Formation of Mixed Self-Assembled Monolayers (SAMs)

Freshly evaporated gold substrates were immersed in deposition solutions made by dissolving the desired ratio of azide-terminated thiol and diluent thiol in ethanol. The total thiol concentration was always 0.1mM. Freshly evaporated gold substrates were then immersed in the deposition solution for 24-36 hours. After deposition, the monolayer-coated samples were rinsed in ethanol and water to remove excess absorbate and dried with N_2 to remove residual solvent. The monolayers were then incubated overnight in an exchange solution made by dissolving 10mM of the diluent thiol in

ethanol. This was done in order to ensure removal of loosely bound azides at defect sites (*S6*).

Immobilization of CcO models onto Self-Assembled Monolayers (SAMs)

Azide-terminated mixed SAM coated gold electrodes were brought into an inert atmosphere glovebox (O_2 concentration< 2ppm) and contacted for 30 minutes with a deposition solution consisting of a 2:1 v:v DMSO/Water mixture containing 200μM copper(II) sulfate TBTA, 400μM sodium ascorbate, 10μM CcO model. The electrodes were then rinsed with copious amounts of DMSO and water and subsequently treated for approximately 1 minute with a 1mM solution of potassium ferricyanide. This was done in order to oxidize the metal centers of our models preventing their reaction with oxygen upon removal from the glovebox. Electrodes were then removed from the glovebox, and rinsed with copious amounts of water. For studies with models **1a** and **2a** (containing copper), the electrodes were treated for approximately 2-3 minutes with a 1 mM solution of copper(II) triflate. For studies with model **2b** (lacking copper), the electrodes were treated for approximately 2-3 minutes with 1M HCl.

Electrochemical measurements:

For gold electrodes on silicon substrates, the electrochemical cell area was defined by pressing down on the sample with a cylindrically bored Teflon™ cone. The bore was filled with electrolyte and a platinum counter electrode and a glass frit-isolated Ag/AgCl/3M NaCl reference electrode were suspended in the cell. Electrochemical measurements using macroscopic planar electrodes were made using an Analog Devices OP27G operational amplifier with a feedback resistor as a current-to-voltage converter.

Another Analog Devices OP27G operation amplifier was used to control the potential between the working and reference electrode. Potential programs were generated using a Wavetek 395 function generator. Current responses were recorded using a Tektronix TDS 520 digital oscilloscope. Measurements were performed at room temperature (~21^{o}C). With the rotating ring-disk electrodes, a commercially purchased Pine AFCBP1 bipotentiostat (Pine Instruments) was used. Rotating ring-disk experiments were performed after inserting the Au-coated Ti disks into commercial ring-disk electrode mounts purchased from PINE (E6 series platinum ring with changeable disk) and were carried out on a Pine AFCBP1 bipotentiostat (Pine Instruments).

Electrochemical Characterization

Characterization of SAMs were performed on planar gold substrates. Electrolyte consisted of 0.1M $NaClO_4$ buffered with 0.019M KH_2PO_4 and 0.031M Na_2HPO_4 (to attain pH 7). Cyclic voltammograms of copper-free models on **S1** or **S2** in the presence of 100mM of dissolved imidazole (pH adjusted to 7 after addition of imidazole) manifest a sharp, reversible couple at 0.15V vs. NHE assigned to the heme Fe(II)/Fe(III) couple. We have used this couple to measure both the standard electron-transfer rate constant, k^0, to the heme as well as the surface coverage of the catalyst (*S6*). The coverage of the catalyst was limited by the coverage of the azide-terminated thiol and kept to approximately 5% of a n-alkane thiol monolayer, less than 40 picomoles/cm^2.

Cyclic voltammograms of the SAMs modified with catalyst **1a** or **2a** in aqueous solutions at pH 7 in the absence of oxygen reveal a broad reversible couple at approximately 0.2V vs. NHE which we assign to both the heme iron and the distal copper.

Treating catalyst **1a** or **2a** coated SAM with dilute acid (1M $HClO_4$) removes copper, which has been verified by a reduction by 50% in the charge in the voltametric peak (cathodic sweep) (Fig. S1).

In air saturated (approximately 0.24mM dioxygen) aqueous solutions buffered at pH 7, the reversible couple disappears, and is replaced by a large current due to catalytic oxygen reduction (Fig. S2). On the slow SAM **S1**, this current begins at approximately 0.3V vs. NHE and increases as the potential becomes more reducing (Fig. S1A). At less reducing potentials (greater than -100mV vs. NHE), the current increases exponentially with potential. This behavior is predicted by Butler-Volmer kinetics for an electrochemical process that is limited by a single electron transfer (*S7*). At more reducing potentials the current dependence on potential is no longer exponential, likely because at higher overpotential mass transfer limits electrocatalysis. In contrast, films of catalyst **1a** on the fast SAM **S2** also catalyze dioxygen reduction starting at the same potential (0.3V vs. NHE) but the current rapidly increases as the potential becomes more reducing until it peaks at -0.08V (Figure S1B), as expected when oxygen becomes depleted at the electrode surface. At strongly reducing potentials the current decreases, reflecting the growing depletion layer adjacent to the electrode.

Rotating Ring-Disk Electrochemistry

Rotating ring-disk electrochemistry was performed using SAMs on gold coated titanium disk electrodes. Electrolyte consisted of 0.1M $NaClO_4$ buffered with 0.019M KH_2PO_4 and 0.031M Na_2HPO_4 (to attain pH 7). The electrolyte was sparged with air for 20 minutes in order to saturate with air. The oxygen concentration was approximately

0.24 mM. The platinum ring (PROS detector) was polished for 1 minute in 0.3 micron alumina slurry (Buehler micropolish A), sonicated in water for 5 minutes, and air dried. An edge-plane graphite disk electrode was used as a standard for the electrochemical reduction of O_2 by two electrons to H_2O_2 against which the collection efficiency of the ring (biased at 0.9V vs. NHE) was determined (*S8*). The graphite disk was immediately replaced with the SAM coated gold electrode, and a ring-disk experiment was performed. This procedure was repeated for every ring-disk experiment. The collection efficiency of the ring was typically between 16-18%. Scans were performed at 0.01V/sec.

Figure S3 displays typical rotating ring-disk experiments for catalyst **1a** on both slow SAM **S1** and fast SAM **S2** (ring current corrected for collection efficiency). The resulting ring current (i_r) can then be ratioed to the simultaneous disk current (i_d) to give a measure of PROS leakage. For all reported data, this ratio was obtained at 0.1V vs. NHE. This potential was chosen as the most positive potential at which there was significant enough current that reproducible measurement could be made. Figure S4 shows typical rotating ring-disk experiments comparing PROS leakage on slow SAM **S1** of catalyst **1a** and **2a**.

Experiments with Tween-20

Catalyst functionalized SAM films were formed on gold disk electrodes as previously described. The electrodes were then immersed in an aqueous solution of tween-20 (5% by weight) for approximately 5 minutes (*S9*). The electrodes were removed from the tween-20 solution, rinsed with water, mounted into the ring-disk assembly, and used immediately.

Figures

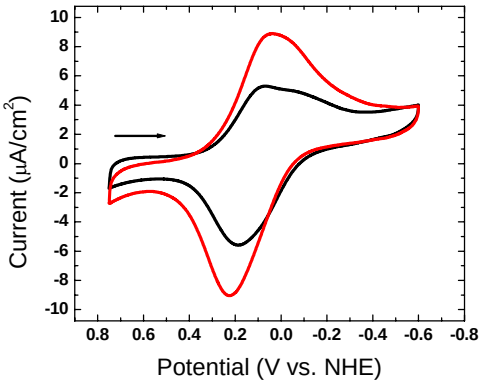

Fig. S1. Cyclic voltammograms of model **2a** (FeCuArOMe) and **2b** (FeArOMe) on the slow SAM **S1**. The scan rate was 0.3V/s. The arrow indicates the start of the scan. Red: after treatment with 1mM solution of copper(II) triflate. Black: after treatment with 1M HCl. Coverage of catalyst is approximately 4.4×10^{-11} mol/cm^2.

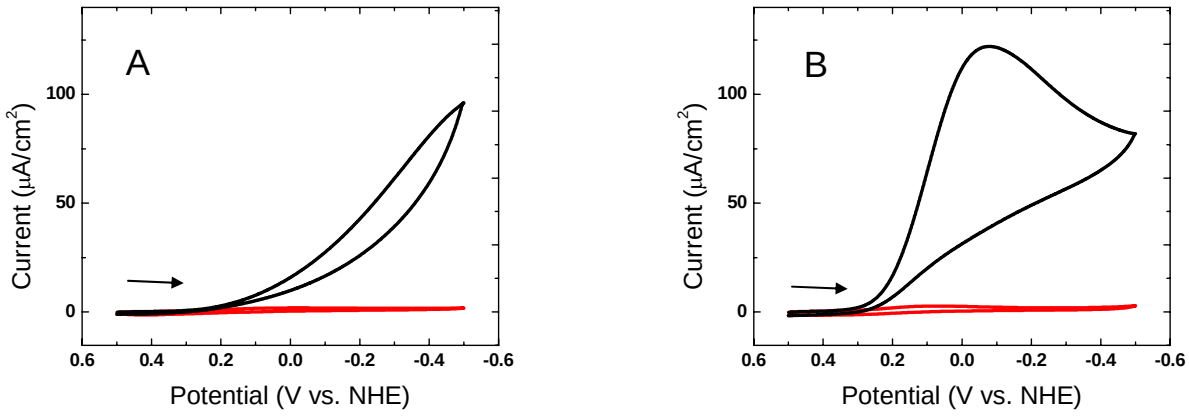

Fig. S2. Cyclic voltammograms of **1a** on either (A) slow SAM **S1** or (B) fast SAM **S2** in electrolyte sparged for 15 minutes with either nitrogen (red) or oxygen (black). The scan rate was 0.05V/sec. Arrow indicates the start of the scan.

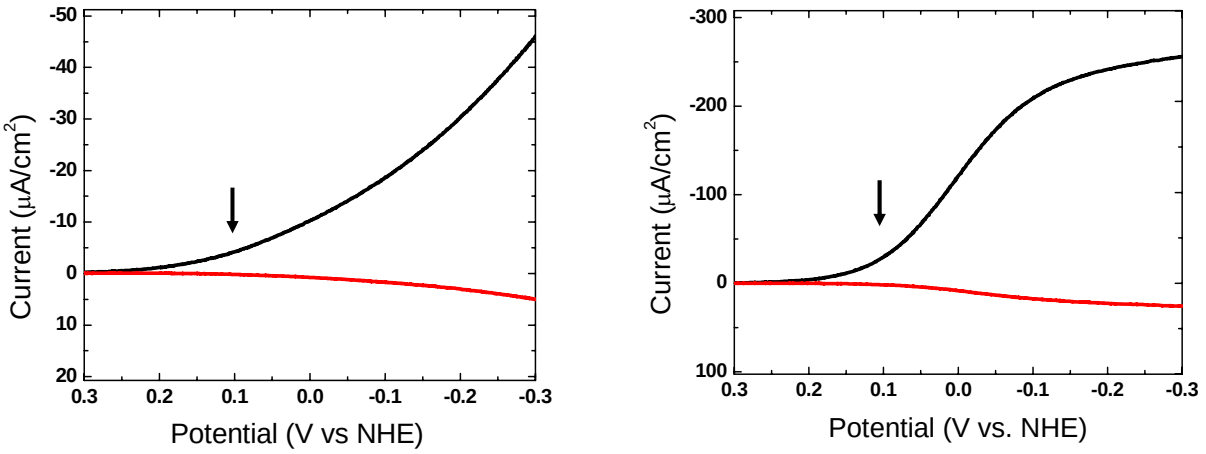

Fig. S3. Typical rotating ring-disk voltammograms of slow SAM **S1** modified with model **1a** (FeCuArOH)**.** Arrow shows the potential at which PROS were measured. The ring was biased at 900mV versus NHE and the current corrected for the collection efficiency of hydrogen peroxide (typically between 16-18%). Data taken in air saturated electrolyte buffered at pH 7. The ring-disk assembly was rotated at 300 rpm.

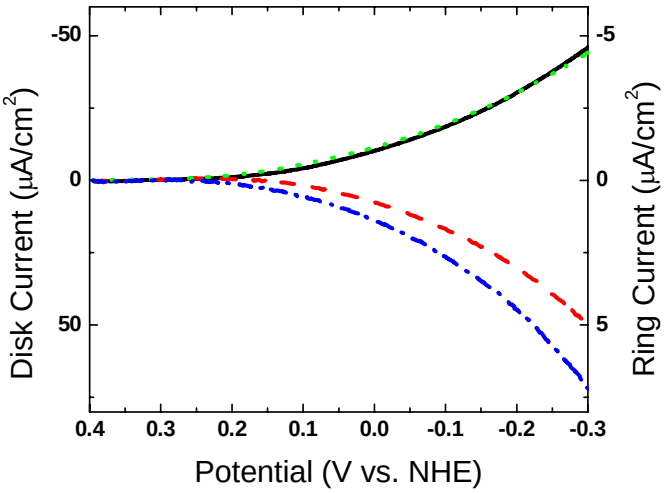

Fig. S4. Typical rotating ring-disk voltammograms of slow SAM **S1** modified with the (FeCuArOH)model **1a** or the (FeCuArOMe) model **2a**. Solid and dotted lines are disk currents for 1a and 2a respectively. Dashed and dash-dotted lines are ring currents for 1a and 2a respectively. Arrow shows the potential at which PROS were measured. The ring was biased at 900mV versus NHE and the current corrected for the collection efficiency of hydrogen peroxide oxidation (typically between 16-18%). Data taken in air saturated electrolyte buffered at pH 7. The ring-disk assembly was rotated at 300 rpm.

References

S1. J. P. Collman, N. K. Devaraj, C. E. D. Chidsey, *Langmuir* **20**, 1051 (2004).

S2. J. P. Collman *et al.*, *Journal of Organic Chemistry* **63**, 8082 (1998).

S3. J. P. Collman, M. Broring, L. Fu, M. Rapta, R. Schwenninger, *Journal of Organic Chemistry* **63**, 8084 (1998).

S4. J. P. Collman, R. A. Decreau, C. Zhang, *Journal of Organic Chemistry* **69**, 3546 (2004).

S5. J. P. Collman, C. J. Sunderland, R. Boulatov, *Inorganic Chemistry* **41**, 2282 (2002).

S6. N. K. Devaraj, R. A. Decreau, W. Ebina, J. P. Collman, C. E. D. Chidsey, *Journal of Physical Chemistry B* **110**, 15955 (2006).

S7. A. J. Bard, L. R. Faulkner, *Electrochemical Methods: Fundamentals and Applications* (John Wiley & Sons, Inc., Hoboken, NJ, ed. Second, 2001), pp.

S8. R. Boulatov, J. P. Collman, I. M. Shiryaeva, C. J. Sunderland, *Journal of the American Chemical Society* **124**, 11923 (2002).

S9. G. B. Sigal, M. Mrksich, G. M. Whitesides, *Langmuir* **13**, 2749 (1997).